




ORIGINAL RESEARCH

Hemodynamic Failure Staging With Blood Oxygenation Level–Dependent Cerebrovascular Reactivity and Acetazolamide-Challenged (^{15}O -) H_2O -Positron Emission Tomography Across Individual Cerebrovascular Territories

Martina Sebök , MD, PhD; Frank van der Wouden , PhD; Cäcilia Mader, MD; Athina Pangalu , MD; Valerie Treyer , PhD; Joseph Arnold Fisher, MD; David John Mikulis , MD; Martin Hüllner , MD; Luca Regli , MD; Jorn Fierstra , MD, PhD; Christiaan Hendrik Bas van Niftrik , MD, PhD

BACKGROUND: Staging of hemodynamic failure (HF) in symptomatic patients with cerebrovascular steno-occlusive disease is required to assess the risk of ischemic stroke. Since the gold standard positron emission tomography-based perfusion reserve is unsuitable as a routine clinical imaging tool, blood oxygenation level–dependent cerebrovascular reactivity (BOLD-CVR) with CO_2 is a promising surrogate imaging approach. We investigated the accuracy of standardized BOLD-CVR to classify the extent of HF.

METHODS AND RESULTS: Patients with symptomatic unilateral cerebrovascular steno-occlusive disease, who underwent both an acetazolamide challenge (^{15}O -) H_2O -positron emission tomography and BOLD-CVR examination, were included. HF staging of vascular territories was assessed using qualitative inspection of the positron emission tomography perfusion reserve images. The optimum BOLD-CVR cutoff points between HF stages 0–1–2 were determined by comparing the quantitative BOLD-CVR data to the qualitative (^{15}O -) H_2O -positron emission tomography classification using the 3-dimensional accuracy index to the randomly assigned training and test data sets with the following determination of a single cutoff for clinical application. In the 2-case scenario, classifying data points as HF 0 or 1–2 and HF 0–1 or 2, BOLD-CVR showed an accuracy of >0.7 for all vascular territories for HF 1 and HF 2 cutoff points. In particular, the middle cerebral artery territory had an accuracy of 0.79 for HF 1 and 0.83 for HF 2, whereas the anterior cerebral artery had an accuracy of 0.78 for HF 1 and 0.82 for HF 2.

CONCLUSIONS: Standardized and clinically accessible BOLD-CVR examinations harbor sufficient data to provide specific cerebrovascular reactivity cutoff points for HF staging across individual vascular territories in symptomatic patients with unilateral cerebrovascular steno-occlusive disease.

Key Words: (^{15}O -) H_2O -PET ■ BOLD ■ cerebrovascular reactivity ■ hemodynamic failure ■ steno-occlusive disease ■ symptomatic stroke

See Editorial by Khaw et al.

Correspondence to: Martina Sebök, MD, PhD, Department of Neurosurgery, University Hospital Zurich, Frauenklinikstrasse 10, 8091 Zurich, Switzerland. Email: martina.seboek@usz.ch

This manuscript was sent to Luciano A. Sposato, MD, MBA, Associate Editor, for review by expert referees, editorial decision, and final disposition.

Supplemental Material is available at <https://www.ahajournals.org/doi/suppl/10.1161/JAHA.123.029491>

For Sources of Funding and Disclosures, see page 11.

© 2023 The Authors. Published on behalf of the American Heart Association, Inc., by Wiley. This is an open access article under the terms of the [Creative Commons Attribution-NonCommercial](https://creativecommons.org/licenses/by-nc/4.0/) License, which permits use, distribution and reproduction in any medium, provided the original work is properly cited and is not used for commercial purposes.

JAHA is available at: www.ahajournals.org/journal/jaha

CLINICAL PERSPECTIVE

What Is New?

- The optimum blood oxygenation level–dependent dependent cerebrovascular reactivity cutoff points for individual hemodynamic failure stages (ie, 0–1–2) were determined by comparing the quantitative blood oxygenation level–dependent cerebrovascular reactivity data to the qualitative (^{15}O -) H_2O - positron emission tomography classification.
- Blood oxygenation level–dependent cerebrovascular reactivity has the accuracy to provide specific hemodynamic failure stage cutoff points for individual cerebrovascular territories.

What Are the Clinical Implications?

- The blood oxygenation level–dependent cerebrovascular reactivity derived cutoff points for individual hemodynamic failure stages may provide a novel imaging approach for future clinical trials investigating the role of revascularization procedures versus medical management in patients with atherosclerotic large vessel occlusion.

Nonstandard Abbreviations and Acronyms

ASL	arterial spin labeling
BOLD	blood oxygenation level–dependent
CBF	cerebral blood flow
cSOD	cerebrovascular steno-occlusive disease
CVR	cerebrovascular reactivity
HF	hemodynamic failure
MCA	middle cerebral artery
NPV	negative predictive value
OEF	oxygen extraction fraction
VUS	volume under the surface

Symptomatic patients with cerebrovascular steno-occlusive disease (cSOD) have an annual risk of 5% to 6% for recurrent acute ischemic events, which may even increase up to 40% in the presence of severe hemodynamic failure.^{1,2} Therefore, reliable and clinically accessible neuroimaging techniques to assess hemodynamic impairment are paramount to inform optimal clinical management. Cerebrovascular reactivity (CVR) is a gradable provocative cerebrovascular response test reflecting severity of hemodynamic failure.^{3–6} Measuring cerebrovascular perfusion reserve

capacity with acetazolamide challenge (^{15}O -) H_2O -positron emission tomography (PET) is considered the benchmark for hemodynamic failure (HF) staging. Severity of HF is divided into 3 stages: Stage 0 represents normal baseline perfusion and normal reserve capacity after an acetazolamide stimulus; Stage 1 represents normal baseline perfusion and impaired perfusion reserve capacity, whereas Stage 2 represents impaired baseline and perfusion reserve capacity and is considered the most severe hemodynamic impairment. Stage 2 is associated with the highest risk for recurrent ischemic events.^{7,8} The largest drawback of the acetazolamide challenge (^{15}O -) H_2O -PET, however, is the cost and high complexity of this specific PET application, which requires an on-site cyclotron in close proximity to the PET scanner. For instance, the daily patient volume at our institute is limited because of competing production of other radiotracers and technical down time, for example, overheating of the cyclotron target.⁹

Magnetic resonance imaging (MRI) methods that can be used to measure resting state blood flow are arterial spin labeling (ASL) and MRI perfusion. Using ASL with a vasoactive stimulus, cerebrovascular reactivity from a direct blood flow measurement can be determined with the added benefit of having a resting cerebral blood flow (CBF) measurement.¹⁰ An emerging form of cerebrovascular reserve testing is blood oxygenation level–dependent cerebrovascular reactivity (BOLD-CVR) functional MRI in combination with a standardized hypercapnic vasoactive stimulus (ie, BOLD-CVR).^{11–14} Assuming the acquisition of the hypercapnia control hardware, the limiting factor is MRI access, which varies with demand and supply. Otherwise, a precise and standardized CO_2 vasoactive stimulus, the BOLD imaging sequence provides stimulus–response CVR data similar to acetazolamide challenge (^{15}O -) H_2O -PET.^{6,15} Furthermore, CO_2 -challenged BOLD-CVR is noninvasive, has lower draw on resources and infrastructure, and is less expensive. The added benefit of the use of a standardized stimulus is the potential for quantitative measurements which may be able to identify quantitative BOLD-CVR criteria to differentiate between HF stages 0–1 and 1–2.^{5,16} Objective HF staging would overcome the disadvantages of the current subjective nature of HF determination (ie, qualitative visual rating).

Here, we report on our study investigating the value of BOLD-CVR to assess HF by comparing measures in the same patients with symptomatic unilateral cSOD, to those measured with a clinical standard of acetazolamide-challenged (^{15}O -) H_2O -PET. Our aim was to use (^{15}O -) H_2O -PET to identify cutoff points from BOLD-CVR for the different HF stages across individual vascular territories.

METHODS

The data used during the current study are available from the corresponding author on reasonable request. This study was performed in line with the principles of the Declaration of Helsinki. Approval was granted by the local research ethics board (KEK-ZH-Nr 2012-0427 & KEK-ZH-Nr 2020-02314). Informed consent was obtained from all individual participants included in the study.

Subjects

This project is part of an ongoing BOLD-CVR study in patients with symptomatic unilateral cSOD. The database consisted of 130 consecutive BOLD-CVR studies in patients with symptomatic unilateral cSOD conducted between 2015 and 2020. As we primarily compared the imaging potential of 2 imaging tools, we included patients with acute and chronic cSOD as well as patients with Moyamoya. Despite a vast difference in the pathophysiology of the included diseases, the HF stages on PET imaging are determined similarly. We selected all subjects over the age of 18 years who underwent both, (^{15}O)- H_2O -PET and BOLD-CVR examination within 6 weeks of each other. Since cSOD tends to have a bilateral appearance in the majority of cases, we followed the NASCET (North American Symptomatic Carotid Endarterectomy Trial) criteria, rating cSOD still to be unilateral if a contralateral stenosis was <50% as graded on carotid ultrasound duplex sonography.¹⁷

We excluded patients with contraindications for MRI, or intolerance to the soft plastic mask or the applied CO_2 stimulus. We also excluded patients with new neurological symptoms or a neurosurgical or endovascular intervention occurring between the 2 methods. Furthermore, patients with bilateral cSOD (bilateral Moyamoya vasculopathy or >50% stenosis on the contralateral side in case of unilateral internal carotid artery/middle cerebral artery (MCA) stenosis/occlusion were also excluded.

MRI Acquisition and Processing BOLD-CVR Maps

MRI data were acquired on a 3-tesla Skyra VD13 (Siemens Healthcare, Erlangen, Germany). During the BOLD MRI sequence, the CO_2 stimulus was modulated by a computer-controlled gas blender with prospective gas targeting algorithms (RespirAct, Thornhill Research Institute, Toronto, Canada).¹⁸ Details about BOLD MRI acquisition and data processing can be found in Data S1.

The CVR calculation¹⁹ included voxel-wise temporal shifting for optimal physiological correlation of the BOLD signal and CO_2 time series. CVR, defined as

the percentage BOLD signal change/mm Hg CO_2 , was then calculated from the slope of a linear least square fit of the BOLD signal time course to the CO_2 time series over the range of the first baseline of 100 seconds, the step portion of the protocol (80 seconds) and the second baseline of 100 seconds on a voxel-by-voxel basis.^{19,20}

PET Acquisition and Processing

All patients received an automated intravenous injection of 371-965 MBq O^{15} -water over 20 seconds per PET scan. During the period of the study, a Discovery STE PET/CT scanner and a Discovery MI PET/CT scanner were in use (GE Healthcare, Waukesha, WI). Details of the PET image analysis can be found in the Data S1. One independent triple board-certified radiologist (nuclear medicine, radiology and neuroradiology) with 10 years of experience assessed the (^{15}O)- H_2O -PET maps (C.M.) for a quantitative PET image analysis to determine the different stages of HF⁶:

Stage 0: normal baseline perfusion and normal perfusion reserve capacity.

Stage 1: normal baseline perfusion and impaired perfusion reserve capacity.

Stage 2: impaired baseline and perfusion reserve capacity.

Statistical Analysis

Normality testing was performed using the Shapiro-Wilk test. All non-normally distributed continuous variables are reported as the median (interquartile range), whereas dichotomous variables are shown as the frequency (%). An independent 2-tailed Student's *t* test was used to compare BOLD-CVR and PET perfusion reserve values within the anterior cerebral artery, middle cerebral artery, and anterior and posterior watershed territory between the individual HF stages (0–1–2, respectively), where $P < 0.05$ was considered statistically significant.

To determine the optimal BOLD-CVR cutoff points between HF stages 0–1 and 1–2 derived from PET perfusion, we followed the method of Skaltsa et al,²¹ by applying a 3-class receiver-operating characteristic-curve analysis that controls for disease prevalence and misclassification costs to our data (Figure 1). We randomly divided the 114 patient observations into a training-set (80% of data points) and test-set (20% of data points) 10000 times. We calculated the volume under the surface (VUS), a 3-dimensional accuracy index, associated with the optimal cutoffs for each vascular territory. Before the VUS analysis, normalization of the BOLD-CVR data was done by Box-Cox power transformation parameter via goodness of fit test²² as the VUS analysis does not allow for negative values. The VUS was optimized by applying a costs-matrix

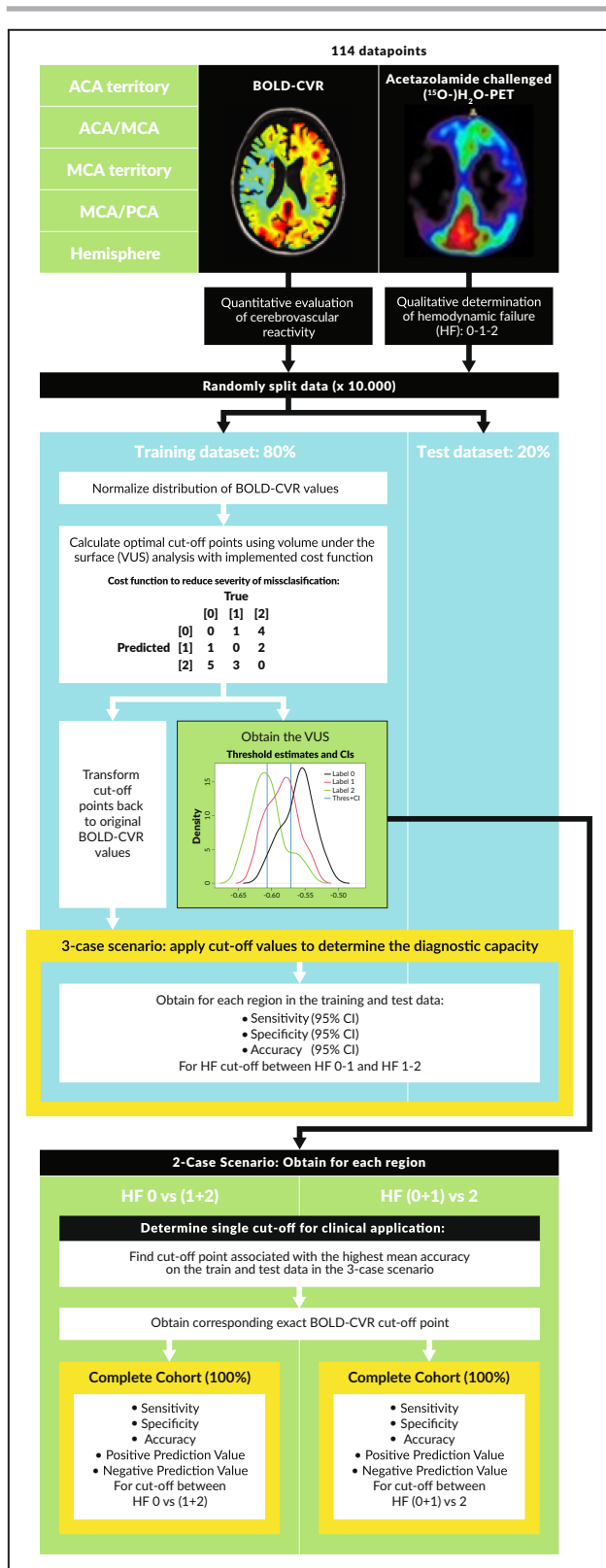


Figure 1. Study analysis flowchart.

In 57 patients with symptomatic cerebrovascular steno-occlusive disease, an acetazolamide-challenged (¹⁵O)-H₂O- positron emission tomography examination was performed within 6 weeks of the blood oxygenation level-dependent-cerebrovascular reactivity examination. Both hemispheres were evaluated separately, and 114 data points were included in this study. The following territories were quantitatively and qualitatively evaluated: anterior cerebral artery, anterior cerebral artery/middle cerebral artery, middle cerebral artery, middle cerebral artery/posterior cerebral artery and the hemisphere. The quantitative evaluation of cerebrovascular reactivity was performed using blood oxygenation level-dependent-cerebrovascular reactivity. Acetazolamide-challenged (¹⁵O)-H₂O-positron emission tomography was used for qualitative determination of HF (HF 0–1–2). By applying a 3-class receiver-operating characteristic-curve analysis, the optimal blood oxygenation level-dependent-cerebrovascular reactivity cutoff points between HF stages 0–1 and HF stages 1–2 derived from the positron emission tomography perfusion study were determined. In total, 114 patient observations were randomly divided into training (80% of data points) and test sets (20% of data points) 10000 times. The volume under the surface, a 3-dimensional accuracy index, associated with the optimal cutoffs for each vascular territory were calculated. The detailed description and analysis pipeline of performed statistical analysis is depicted in the *Materials and Methods (2.4 Statistical analysis)*. Using these cutoffs, the overall blood oxygenation level-dependent-cerebrovascular reactivity diagnostic capacity (accuracy, sensitivity, and specificity) for each territory were determined. The cutoff points with the maximum average accuracy in the training and test sets were chosen in the 3-case scenario. In a clinical setting discriminating between HF stages 0 and 1–2 or HF stages 0–1 and 2 can be of interest (ie, the 2-case scenario). These cutoff points and predictive values are presented in this manuscript. ACA indicates anterior cerebral artery; BOLD, blood oxygenation level-dependent; CVR, cerebrovascular reactivity; HF, hemodynamic failure stage; MCA, middle cerebral artery; PCA, posterior cerebral artery; PET, positron emission tomography; and VUS, volume under the surface.

misclassification). In this scenario the cost of misclassifying a patient exhibiting HF 2 as having HF 0 was deemed the most serious error and was given a 5. The inverse (ie, false positive classification of HF 2 when none is present [HF 0]) was also considered severe and classified as 4. Classifying a patient with HF 1 as 2 was given a cost value 3, whereas classifying a patient with HF 2 as 1, a cost value 2 was given. Lastly, classifying a patient with HF 1 as 0 and HF 0 as 1, a cost value of 1 was given. A cost function of 0 was given to all correct classifications.

This exercise provides 10000 optimal cutoff points between HF 0–1 and HF 1–2 for each vascular territory. Using these cutoffs, we determined the overall BOLD-CVR diagnostic capacity (accuracy, sensitivity, and specificity) for each territory. We chose the cut-off points with the maximum average accuracy in the training and test sets.

In a clinical setting discriminating between HF stages 0 and 1–2 or HF stages 0–1 and 2 can be of

for misclassification with values ranging from 0 to 5 as determined by interdisciplinary clinical consensus (where 0 is the least severe, and 5 the most severe

interest. We therefore evaluated the diagnostic capacities of the BOLD-CVR cutoff points in this scenario separately. Cases were grouped as HF 0 or HF 1–2 to determine the diagnostic capacity of the HF 0 versus 1–2 cutoff point, and HF 0–1 or HF 2 to determine the diagnostic capacity of the HF 0–1 versus 2 cutoff point. For each territory, we repeated our random shuffling exercise, obtained the optimal cutoff points, recorded the VUS, and selected the 2 BOLD-CVR cutoff points based on the maximum average accuracy of the training- and test-set. After a random shuffling, the analysis on each of the territories was performed before the next shuffling. We applied these cutoff points to the complete data set to create a 2x2 table and determine the predictive value of each cutoff point. All statistical analyses were performed using Microsoft R Open 4.0.2 (Microsoft R Core Team, 2020).

RESULTS

Study Population Characteristics

Fifty-seven data sets from 53 patients (54.3 [20.8] years; 71.7% males) with symptomatic unilateral cSOD were included in the analysis, generating 114 data points (ipsilateral+contralateral hemisphere). Four subjects underwent (¹⁵O)-H₂O-PET and BOLD-CVR examination on 2 occasions (as part of routine follow-up imaging). The inclusion of the repeated studies did not modify the results of the study. A patient flow diagram can be reviewed in [Figure S1](#).

The included 53 patients presented with following pathologies: 28 patients with internal carotid artery occlusion, 5 patients with MCA occlusion, 1 patient with internal carotid artery stenosis, 3 patients with MCA stenosis and 16 patients with Moyamoya disease. The mean time between the BOLD-CVR and (¹⁵O)-H₂O-PET scans was 18±14 days. 41.5% of patients were smokers, 52.8% were treated with oral medication because of hypertension, and 37.7% because of hypercholesterolemia. 26.4% of patients were obese, and 17% had diabetes. In 3.8% of patients a positive family history for cerebral ischemic events existed, and 39.6% of patients suffered a previous ischemic event or a bleeding ([Table S1](#)).

An overview of the BOLD-CVR findings and PET perfusion reserve measurements for the whole brain, hemispheres, and vascular territories are presented in [Table 1](#). [Figure 2](#) shows the boxplot distribution between qualitative PET-derived HF stages and quantitative BOLD-CVR values for the whole hemisphere, anterior cerebral artery (ACA) and MCA territories, and both watershed territories. Here, significant BOLD-CVR differences between different HF stages in all territories are seen, except between HF stages 0 and 1 of the anterior watershed (ACA/MCA territory).

Table 1. BOLD-CVR and PET Perfusion Reserve Findings

	PET	BOLD
	Perfusion reserve, mL/100mg tissue per min, median (IQR)	CVR, %BOLD signal change/mmHg CO ₂ , median (IQR)
Whole brain	0.15 (0.10)	0.15 (0.09)
Ipsilateral hemisphere*	0.14 (0.09)	0.11 (0.11)
Contralateral hemisphere	0.16 (0.09)	0.17 (0.10)
Vascular territories		
Anterior vascular territories		
Ipsilateral* ACA territory	0.15 (0.10)	0.11 (0.09)
Contralateral ACA territory	0.16 (0.09)	0.15 (0.10)
Ipsilateral* MCA territory	0.11 (0.10)	0.07 (0.12)
Contralateral MCA territory	0.16 (0.10)	0.17 (0.10)
Anterior and posterior watershed territories		
Ipsilateral* ACA/MCA territory	‡	0.09 (0.11)
Contralateral ACA/MCA territory	‡	0.15 (0.10)
Ipsilateral* MCA/PCA territory	‡	0.11 (0.10)
Contralateral MCA/PCA territory	‡	0.16 (0.10)

ACA indicates anterior cerebral artery; BOLD, blood oxygenation level-dependent; CBF, cerebral blood flow (mL/100 mg tissue per minute); CVR, cerebrovascular reactivity defined as percentage BOLD signal change per mmHg CO₂; IQR, interquartile range; MCA, middle cerebral artery; PCA, posterior cerebral artery; and PET, positron emission tomography.

*The ipsilateral hemisphere/territory is considered the hemisphere/territory on the side of vessel pathology.

‡Because of technical reasons, the positron emission tomography perfusion reserve for the watershed territories cannot be calculated.

Quantitative BOLD-CVR values are presented in [Table S2](#).

Three-Case Scenario to Evaluate Overall BOLD-CVR Diagnostic Capacity

We defined a 3-case scenario (separating HF stages 0–1–2) to evaluate the overall diagnostic capacity of BOLD-CVR. For the 3-case scenario, the volume under the surface curves for all vascular territories can be reviewed in [Figure 3](#). The corresponding class based predictive values from the 3-case scenario are depicted in [Table S3](#).

In the 3-case scenario, BOLD-CVR performs best for the MCA territory with approximately two-thirds of cases across the 3 classes classified correctly, followed by the ACA territory and anterior watershed. The most clinically relevant HF stage classification is for the MCA territory, and here we see a high specificity and negative predictive value for all 3 stages, with the highest values for the most clinically relevant HF stage, stage 2. The specificity and negative predictive value for HF stage 2 are also high for the other 3 territories

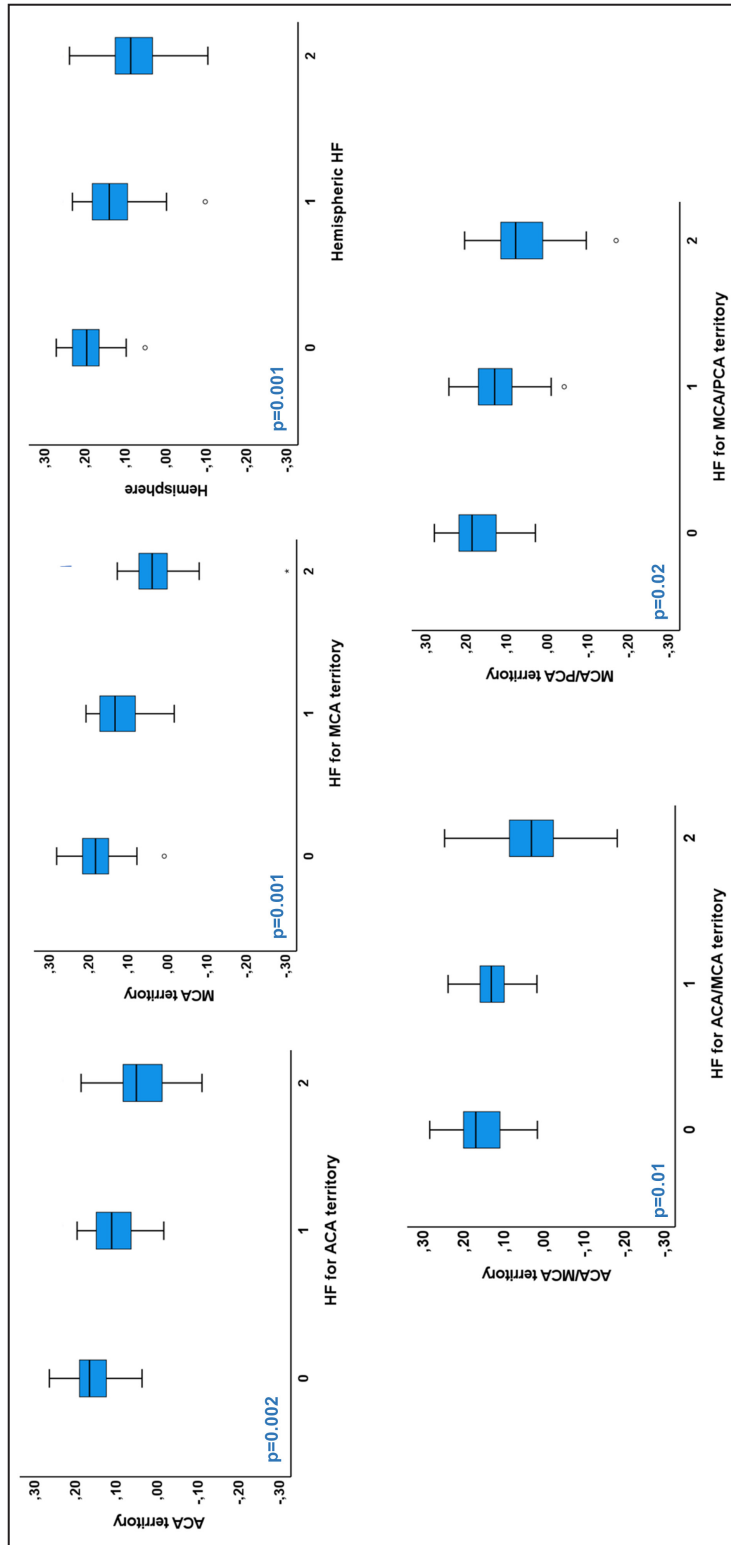


Figure 2. Boxplot distribution for each vascular territory.

The boxplot distribution between qualitative positron emission tomography-derived hemodynamic failure stages and quantitative blood oxygenation level-dependent cerebrovascular reactivity values for the whole hemisphere, anterior cerebral artery, and middle cerebral artery territories as well as both watershed territories. The box of the box and whisker plots represents the median value with interquartile range (25th–75th percentile). The upper and lower whiskers represent values outside the middle 50% (ie, the values below the 25th and above the 75th percentile). ANOVA was used to calculate differences among the 3 groups (hemodynamic failure 0–1–2). To avoid Type I error for multiple comparison, Bonferroni correction was applied. Significant blood oxygenation level-dependent cerebrovascular reactivity differences between different hemodynamic failure stages are seen in all territories. ACA indicates anterior cerebral artery; HF, hemodynamic failure stage; MCA, middle cerebral artery; and PCA, posterior cerebral artery.

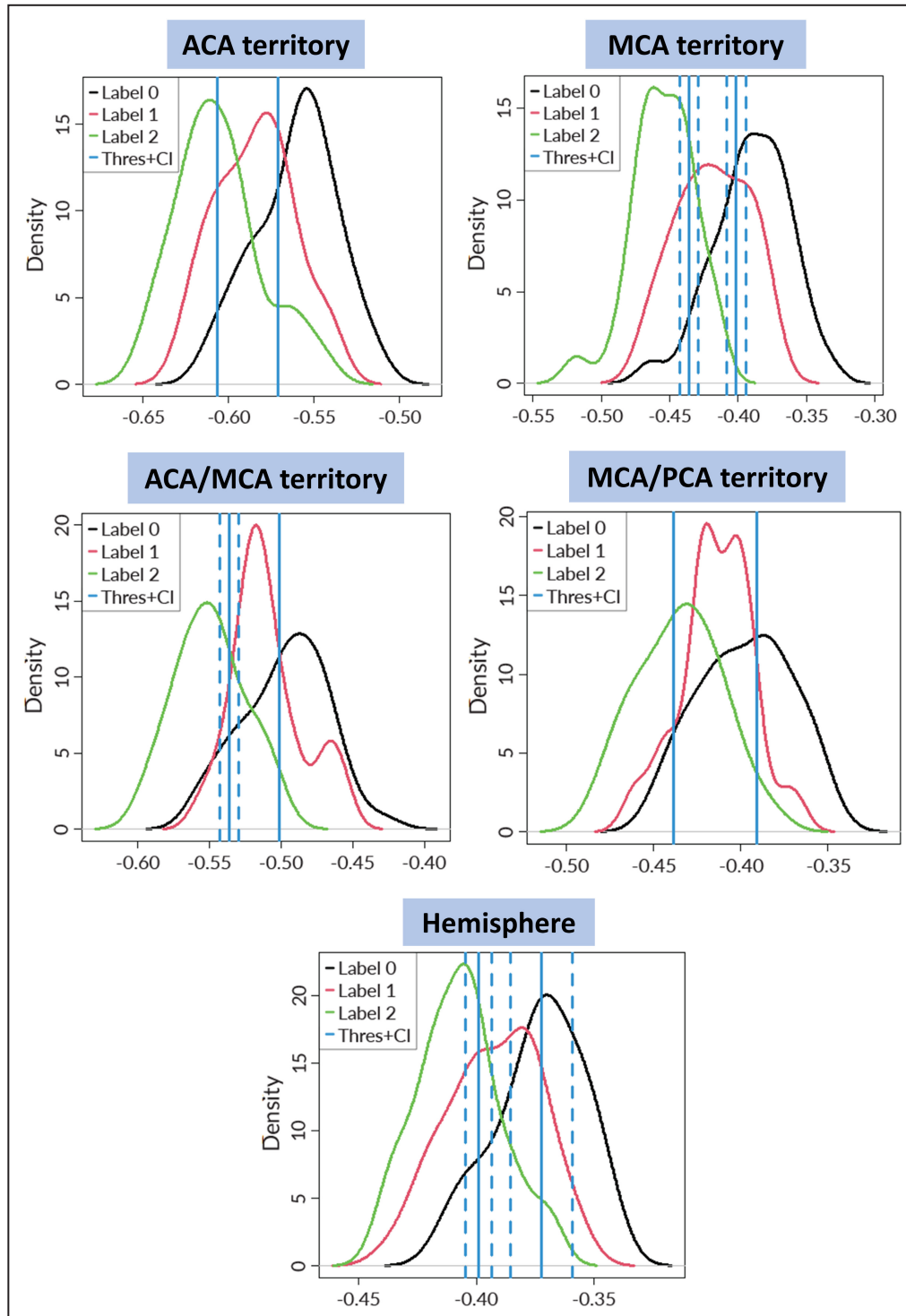


Figure 3. Volume under the surface curves for all vascular territories.

The volume under the surface distribution for the whole hemisphere, anterior cerebral artery, and middle cerebral artery territories as well as both watershed territories is shown in this figure, with threshold estimates and CIs. Label 0 describes hemodynamic failure 0; label 1, hemodynamic failure 1; and label 2, hemodynamic failure 2. The solid blue line indicates the threshold, with the dashed blue line showing the CI. In some figures, the dashed blue line is not clearly displayed because of its proximity to the solid blue line. The BOLD-CVR values presented on the x-axis are normalized. (See Figure 1). ACA indicates anterior cerebral artery; HF, hemodynamic failure stage; MCA, middle cerebral artery; and PCA, posterior cerebral artery.

Downloaded from <http://ahajournals.org> by on December 26, 2023

and the hemisphere. Sensitivity and positive predictive value across the territories and HF stages present with larger variations in the 3-case classification, with the highest values for HF stage 2 of the MCA territory.

Two-Case Scenario for Clinical Application

For the clinically useful diagnostic capacity of BOLD-CVR, we defined a 2-case scenario looking at cutoff points for HF stage 0–1, and 1–2. In the 2-case scenario, classifying data points as HF 0 or 1–2 and HF 0–1 or 2, BOLD-CVR showed an accuracy of >0.7 for all vascular territories for HF 1 and HF 2 cutoff points. Table 2 shows the defined cutoffs for clinical application between HF stage 0 and 1 and their predictive values. Similarly, the defined cutoffs for vascular territories to differentiate between HF stages 1 and 2 with predictive values are presented in Table 3. In particular, the MCA territory had an accuracy of 0.79 for HF 1 and 0.83 for HF 2, whereas the ACA had an accuracy of 0.78 for the HF 1 and 0.82 for HF 2. The cutoff points between HF stages 1 and 2 for all vascular territories show better sensitivity and positive predictive value when compared with cutoff points between HF stages 0 and 1. The classification table for the 3-case scenario (confusion matrix) can be reviewed in Table S4.

DISCUSSION

The main findings of this study are that BOLD-CVR, determined using a standardized CO₂ challenge and BOLD changes has the accuracy to provide specific HF stage cutoff points for different vascular territories. We found that the MCA territory to be the most consistent territory, with a high accuracy for both the 3-case and clinical 2-case scenarios. Most importantly, the capacity for HF stage 2 is high, in both the 2-case and 3-case scenario, making BOLD-CVR a reliable tool to identify the clinically relevant HF stage 2. The cutoff points for HF stage 2 in the 2-case, *clinical*, scenario, provide high sensitivity and positive predictive value for HF.

The overall accuracy of the anterior and posterior watershed areas was lower than that of the MCA and ACA territories, both in the 2-case and 3-case scenarios. This is most likely because of the difference in the anatomical location and variability of vascular distribution in watershed areas between patients, which cannot be corrected by data normalization. As expected, the data averaged over a hemisphere showed the lowest diagnostic power. It is the largest region and was classified based on the vascular territory with the worst HF stage. Interestingly, the HF stage 2 hemispheric cutoff point of 0.1041 exactly corresponds to

Table 2. Defined Clinical BOLD-CVR Cutoff Points Between HF Stage 0 and 1–2

BOLD-CVR	Cutoff HF 0–1	Sensitivity (95% CI)	Specificity (95% CI)	PPV (95% CI)	NPV (95% CI)	Positive LR (95% CI)	Negative LR (95% CI)	Accuracy (95% CI)
ACA	0.1321	0.7308 (0.5975–0.8323)	0.7581 (0.6385–0.8475)	0.7170 (0.5843–0.8203)	0.7705 (0.6509–0.8581)	3.021 (1.954–5.205)	0.355 (0.199–0.537)	0.7456 (0.6555–0.8225)
MCA	0.1669	0.6154 (0.4590–0.7511)	0.8800 (0.7874–0.9356)	0.7273 (0.5578–0.8493)	0.8148 (0.7167–0.8844)	5.128 (2.814–11.830)	0.437 (0.266–0.623)	0.7895 (0.7031–0.8602)
ACA-MCA	0.1677	0.4000 (0.2702–0.5455)	0.8986 (0.8051–0.9500)	0.7200 (0.5242–0.8572)	0.6966 (0.5946–0.7824)	3.943 (1.906–11.300)	0.668 (0.493–0.832)	0.7018 (0.6089–0.7838)
MCA-PCA	0.1734	0.5227 (0.3794–0.6625)	0.8571 (0.7566–0.9205)	0.6970 (0.5266–0.8262)	0.7407 (0.6360–0.8237)	3.659 (2.006–7.946)	0.557 (0.378–0.740)	0.7281 (0.6367–0.8072)
Hemisphere	0.1881	0.5405 (0.3838–0.6896)	0.8701 (0.7772–0.9279)	0.6667 (0.4878–0.8077)	0.7976 (0.6996–0.8696)	4.162 (2.189–8.777)	0.528 (0.337–0.719)	0.7632 (0.6744–0.8378)

ACA indicates anterior cerebral artery; BOLD, blood oxygenation level–dependent; CVR, cerebrovascular reactivity defined as percentage BOLD signal change per mm Hg CO₂; HF, hemodynamic failure; LR, likelihood ratio; MCA, middle cerebral artery; NPV, negative predictive value; PCA, posterior cerebral artery; and PPV, positive predictive value.

Table 3. Defined Clinical BOLD-CVR Cutoff Points Between HF Stage 0–1 and 2

BOLD-CVR	Cutoff HF 1–2	Sensitivity (95% CI)	Specificity (95% CI)	PPV (95% CI)	NPV (95% CI)	Positive LR (95% CI)	Negative LR (95% CI)	Accuracy (95% CI)
ACA	0.0444	0.9101 (0.8325–0.9537)	0.5200 (0.3350–0.6997)	0.8710 (0.7879–0.9246)	0.6190 (0.4088–0.7925)	5.785 (2.822–15.459)	0.527 (0.306–0.743)	0.8246 (0.7421–0.8894)
MCA	0.0776	0.8462 (0.7501–0.9097)	0.8056 (0.6497–0.9025)	0.9041 (0.8150–0.9528)	0.7073 (0.5552–0.8239)	5.236 (3.186–10.006)	0.230 (0.093–0.403)	0.8333 (0.7520–0.8966)
ACA-MCA	0.0604	0.9012 (0.8170–0.9491)	0.6970 (0.5266–0.8262)	0.8795 (0.7922–0.9332)	0.7419 (0.5675–0.8630)	7.057 (3.828–17.836)	0.336 (0.169–0.522)	0.8421 (0.7620–0.9037)
MCA- PCA	0.0661	0.8721 (0.7853–0.9271)	0.4643 (0.2953–0.6419)	0.8333 (0.7431–0.8963)	0.5417 (0.3507–0.7211)	3.630 (1.786–7.775)	0.614 (0.394–0.831)	0.7719 (0.6840–0.8453)
Hemisphere	0.1041	0.7600 (0.6522–0.8425)	0.6667 (0.5098–0.7937)	0.8143 (0.7077–0.8881)	0.5909 (0.4441–0.7231)	2.778 (1.781–4.646)	0.439 (0.245–0.653)	0.7281 (0.6367–0.8072)

ACA indicates anterior cerebral artery; BOLD, blood oxygenation level–dependent; CVR, cerebrovascular reactivity, defined as percentage BOLD signal change per mmHg CO₂; HF, hemodynamic failure; LR, likelihood ratio; MCA, middle cerebral artery; NPV, negative predictive value; PCA, posterior cerebral artery; and PPV, positive predictive value.

the BOLD-CVR values found in a previous study using a BOLD-CVR hemispheric cutoff point of an average of a healthy cohort minus 2 SDs.¹⁵

Hemodynamic Failure Staging: an Ongoing Search for an Optimal Imaging Technique

Hemodynamic failure stages were originally defined using PET techniques with autoregulatory vasodilation as characteristic of HF stage 1 and autoregulatory failure as HF stage 2.²³ In patients with reduced cerebral perfusion pressure attributable to diminished cerebral inflow, there are 2 main compensatory responses: (1) autoregulation with vasodilation of downstream resistance arterioles, and (2) increased oxygen extraction fraction (OEF).²⁴ All CVR investigation tools require a vasodilatory stimulus and paired flow studies as defined by Derdeyn²⁵ to assess the vascular reserve.

Historically, HF assessment using CVR was done using direct CBF measurements generated with (¹⁵O)-H₂O-PET or ¹³³Xenon-single-photon emission computed tomography.^{4,26} Characteristic of PET-CVR and single-photon emission computed tomography-CVR studies is the steady-state investigation of perfusion reserve, which requires 3 steps: (1) cerebral blood flow measurement before vasoactive stimulus, (2) cerebral blood flow measurement after vasoactive stimulus, and (3) a difference (ie, perfusion reserve) map.

Specifically for (¹⁵O)-H₂O-PET, the examination can be easily performed with a single dose acetazolamide injection,^{27,28} the examination requires minimal subject cooperation, and the evaluation of CVR is sensitive for pathological values and has a spatial resolution of 3 mm.⁹ The disadvantages of the (¹⁵O)-H₂O-PET examination are the limited clinical availability because of the need for close proximity of the cyclotron and PET scanner, the higher costs compared with MR imaging, and the need for a radioactive tracer. Moreover, acetazolamide takes at least 20 minutes to have a vasodilatory effect, the effect is not quantifiable, and vasoconstriction can still occur with hyperventilation.^{27,29} Furthermore, using PET quantitatively would require the use of a direct arterial line that allows for a direct arterial sampling which allows for a direct and quantitative CBF measurement. This is only an inferred stimulus and suboptimal in patients with steno-occlusive disease, which makes PET only a semi-quantitative imaging method.^{30,31}

In contrast, a standardized CO₂ challenge BOLD-CVR investigation will result in quantitative and reproducible CVR measurements, enabling comparison of CVR studies in single patients to those from an atlas of healthy people,³² repeat studies in a single patient over

time³³ and cohort studies between centers.³⁴ There is no need for radiation, an external tracer or contrast agent and with the use of CO₂, the vascular stimulus can be terminated abruptly after the end of the study or sooner if necessary.^{18,35}

Other MRI methods that can be used to measure resting state blood flow are ASL and MRI Perfusion. Using ASL with a vasoactive stimulus, cerebrovascular reactivity from a direct blood flow measurement can be determined with the added benefit of having a direct resting cerebral blood flow measurement using radiofrequency pulses to magnetically label the water molecules that are then used as an endogenous tracer for the measurement of CBF. However, there are important disadvantages of the ASL technique as the low signal-noise ratio, several types of artifacts, limited spatial resolution, impossible quantification of the tissue blood volume and still pending automation and standardization.¹⁰ As far as we know, MR perfusion has not been used to determine perfusion changes as it would also require a double dosage of contrast with a break to washout the gadolinium used during the first investigation. It could however function as a perfect study to corroborate the BOLD-CVR findings.

BOLD-CVR Versus (¹⁵O-) H₂O-PET: Complementary Techniques for Hemodynamic Failure Staging?

Our findings add a novel quantitative perspective to CVR assessment using BOLD by providing specific BOLD-CVR threshold for the 3 different HF stages. This helps to overcome a major current limitation of BOLD-CVR. Contrary to PET-CVR and single-photon emission computed tomography-CVR studies, the BOLD-CVR examination is a dynamic study of cerebral hemodynamic status and currently it cannot provide information about the resting cerebral blood flow. This means that without precise cutoff points, BOLD-CVR measurements lack the necessary baseline investigations of cerebral blood flow to characterize the different HF stage.⁶ Therefore, our aim was to quantify the BOLD-CVR HF cutoff points using (¹⁵O-)H₂O-PET investigation for initial classification. We show the potential of BOLD-CVR to have predefined threshold for HF stages 1 and 2 of the ACA and MCA territories, as well as for both watershed territories in patients with symptomatic unilateral cSOD, who underwent both, (¹⁵O-)H₂O-PET perfusion reserve measurements and quantitative BOLD-CVR measurements. Interestingly, there are attempts to derive resting CBF measurements from BOLD functional imaging studies using a hypoxia-induced bolus of deoxyhemoglobin as an alternative noninvasive gadolinium tracer.³⁶

To our knowledge, currently only the JET-2 (Japanese Extracranial-Intracranial Bypass Trial-2) has suggested

specific CVR thresholds for HF stages but only for the HF stage 2. Here, a single-photon emission computed tomography-CVR threshold of <10% CVR was proposed, as they showed that patients with CVR values below that threshold are as likely to develop a recurrent ischemic stroke event as patients who lacked a CVR increase at all (ie, CVR <0%).^{37,38} Similarly to their findings, none of our BOLD-CVR cutoff points were below 0.

Other studies introduced increased OEF to determine a specific cutoff point for HF stage 2^{39,40} and recognized the importance of setting thresholds for identifying compromised cerebral hemodynamics. These studies used a threshold of the outer limits of the range in a group of 18 control subjects; 11 of the 13 patients with ipsilateral recurrent strokes had increased OEF, as defined by this threshold.^{3,39} As OEF only increases in HF stage 2, this would have restricted the OEF range (too small an SD) to allow for adequate detection. Therefore, in the later COSS (Carotid Occlusion Surgery Study), this cutoff point resulted in average recurrent stroke rate of ~20%, far below their expected rate of ~40%.⁴¹ Therefore, it is not surprising that other studies deemed an increased cerebral blood volume as an additional parameter to define HF stage 2.^{3,24} This, however, limits the use of increased OEF as the primary HF stage 2 marker.

Future Directions

Although the COSS study⁴² and JET-2 study³⁸ did provide thresholds for HF stage 2, attributable to the semi-quantitative nature of the used imaging techniques, until now no clinically relevant quantitative threshold for HF has been described. In this regard, BOLD-CVR may provide clinically relevant cutoff points for HF staging, whereas our next step is a multicenter validation of the presented quantitative BOLD-CVR thresholds. Furthermore, the future aim should be a prospective randomized multicentric trial including patients who underwent BOLD-CVR after a large artery occlusion and either unsuccessful or successful thrombectomy to assess (persisting) HF.⁴³ Using BOLD-CVR derived quantitative HF cutoffs, patients with HF stage 2 can be randomized into surgical and medical groups and followed-up. Lastly, as mentioned above, work is proceeding to derive resting cerebral hemodynamic measurement from BOLD functional MRI investigation using deoxyhemoglobin as a susceptibility contrast agent.³⁶ This would open the door for much wider applications of BOLD imaging and could mean a paradigm shift in clinical value of hemodynamic imaging in patients with cSOD.

Limitations

This is a retrospective analysis of prospectively collected data from single-center tertiary neuroscience

center. The patient population is heterogeneous, including unilateral intra- and extracranial cSOD, including unilateral Moyamoya vasculopathy. The difference in pathophysiology and CVR patterns between etiologies as well as timing after stroke could have influenced the results; however, our aim was not to investigate different cerebrovascular pathologies. Our aim was to evaluate the potential of BOLD-CVR to detect HF. Although the pathophysiology between unilateral intra- and extracranial cSOD, especially for patients with Moyamoya disease are vastly different, PET HF investigations are evaluated independently of the underlying pathology and the used HF principles do not differ between both pathologies. Therefore, we deemed it adequate to combine these patient groups. Secondly, until now, (¹⁵O-)-H₂O-PET has not been used as a primary cerebrovascular hemodynamic measurement of the cerebrovascular reserve in a clinical trial, partly also because of the difficulty of obtaining (¹⁵O-)-H₂O-PET images. Therefore BOLD-CVR, being available on every MRI scanner, could be an useful alternative for (¹⁵O-)-H₂O-PET.⁶ Thirdly, although the overall difference between the different stages measured with BOLD-CVR is clear, there is an overlap in density plots. This could be attributable to an intrinsic difference between BOLD-CVR and (¹⁵O-)-H₂O-PET, which needs to be further studied to understand the clinical value of these changes. Furthermore, although the diagnostic capacities of BOLD-CVR for all stages was good, and in some vascular territories it was excellent, there are some major outliers that need further investigation to determine which technique yields the most clinically valid results. To obtain these results, a standardized hypercapnia challenge was necessary,¹⁸ which makes this technique currently not widely available. However, using a standardized computer-controlled gas blender with prospective gas targeting algorithms allows to produce the same stimulus in every patient, using a CO₂ stimulus of 10 mmHg as a supramaximal stimulus, while this might not be the case for a stimulus of 5 mmHg causing an overestimation of the CVR if using a 5 mmHg stimulus. Moreover, evaluating CVR without the correction for CO₂ but for instance with an ipsi- versus contralateral analysis or an analysis against the cerebellum like in the JET-2 and COSS study, would make the CVR measurement semi-quantitative. This would result in the same bias of the other studies and it does not correct for the differences in stimulus. The disadvantage of the BOLD-CVR technique is that the quantitative CVR derived from BOLD MRI is only an indirect measurement of perfusion reserve and not a direct measurement of cerebral blood flow. Previous paper by our group¹⁹ demonstrated an improvement of the sensitivity and reliability of quantitative CVR measurements using iterative decomposition and novel

determination of different components of the dynamic CO₂-BOLD relationship. Important to mention is that the diagnostic capability of BOLD-CVR is greatest in the differentiation between the HF 0–1 and HF 2. Our cohort constituted of more patients suspected of having HF stage 1 or 2 than a general stroke population would, which would result in more misclassifications in a general population (ie, spectrum bias). However, tests like BOLD-CVR and (¹⁵O-)-H₂O-PET are only indicated with suspected HF and therefore our cohort most likely represents an adequate cohort of patients with stroke undergoing such tests. Last, to assess its validity, these new BOLD-CVR measurements needs to be validated with important end points like recurrent stroke to determine its true accuracy and clinical relevance.^{44,45}

CONCLUSIONS

Standardized and clinically accessible BOLD-CVR examinations harbor sufficient data to provide specific cerebrovascular reactivity cutoff points for HF staging across individual vascular territories in symptomatic patients with unilateral cerebrovascular steno-occlusive disease.

ARTICLE INFORMATION

Received May 10, 2023; accepted September 11, 2023.

Affiliations

Department of Neurosurgery (M.S., L.R., J.F., C.H.v.N.) and Clinical Neuroscience Center (M.S., A.P., L.R., J.F., C.H.v.N.), University Hospital Zurich, University of Zurich, Switzerland; Department of Geography, University of Hong Kong, China (F.v.d.W.); Department of Nuclear Medicine (C.M., V.T., M.H.) and Department of Neuroradiology (A.P.), University Hospital Zurich, University of Zurich, Switzerland; Department of Anesthesia and Pain Management, University Health Network, Toronto, Ontario, Canada (J.A.F.); Institute of Medical Science, University of Toronto, Toronto, Ontario, Canada (J.A.F., D.J.M.); and Joint Department of Medical Imaging and the Functional Neuroimaging Laboratory, University Health Network, Toronto, Ontario, Canada (D.J.M.).

Sources of Funding

This work was supported by the Clinical Research Priority Program of the University of Zurich (UZH CRPP Stroke).

Disclosures

J.A.F. and D.J.M. contributed to the development of the RespirAct used in this study and have equity in the company. The remaining authors have no disclosures to report.

Supplemental Material

Data S1
Tables S1–S4
Figure S1
References^{19,46–48}

REFERENCES

- Barnett HJM, Taylor DW, Haynes RB, Sackett DL, Peerless SJ, Ferguson GG, Fox AJ, Rankin RN, Hachinski VC, Wiebers DO, et al. Beneficial effect of carotid endarterectomy in symptomatic patients

- with high-grade carotid stenosis. *N Engl J Med*. 1991;325:445–453. doi: [10.1056/nejm199108153250701](https://doi.org/10.1056/nejm199108153250701)
2. Klijn CJ, Kappelle LJ, Algra A, van Gijn J. Outcome in patients with symptomatic occlusion of the internal carotid artery or intracranial arterial lesions: a meta-analysis of the role of baseline characteristics and type of antithrombotic treatment. *Cerebrovasc Dis*. 2001;12:228–234. doi: [10.1159/000047708](https://doi.org/10.1159/000047708)
 3. Derdeyn CP, Grubb RL Jr, Powers WJ. Re: stages and thresholds of hemodynamic failure. *Stroke*. 2003;34:589. doi: [10.1161/01.Str.0000058161.89420.F4](https://doi.org/10.1161/01.Str.0000058161.89420.F4)
 4. Powers WJ, Zazulka AR. PET in cerebrovascular disease. *PET Clin*. 2010;5:83–106. doi: [10.1016/j.cpet.2009.12.007](https://doi.org/10.1016/j.cpet.2009.12.007)
 5. Powers WJ. Cerebral hemodynamics in ischemic cerebrovascular disease. *Ann Neurol*. 1991;29:231–240. doi: [10.1002/ana.410290302](https://doi.org/10.1002/ana.410290302)
 6. Fierstra J, van Niftrik C, Warnock G, Wegener S, Piccirelli M, Pangalu A, Esposito G, Valavanis A, Buck A, Luft A, et al. Staging hemodynamic failure with blood oxygen-level-dependent functional magnetic resonance imaging cerebrovascular reactivity: a comparison versus gold standard ((15)O)-H₂O-positron emission tomography. *Stroke*. 2018;49:621–629. doi: [10.1161/strokeaha.117.020010](https://doi.org/10.1161/strokeaha.117.020010)
 7. Reynolds MR, Derdeyn CP, Grubb RL Jr, Powers WJ, Zipfel GJ. Extracranial-intracranial bypass for ischemic cerebrovascular disease: what have we learned from the carotid occlusion surgery study? *Neurosurg Focus*. 2014;36:E9. doi: [10.3171/2013.10.Focus13427](https://doi.org/10.3171/2013.10.Focus13427)
 8. Derdeyn CP, Gage BF, Grubb RL Jr, Powers WJ. Cost-effectiveness analysis of therapy for symptomatic carotid occlusion: PET screening before selective extracranial-to-intracranial bypass versus medical treatment. *J Nucl Med*. 2000;41:800–807.
 9. Treyer V, Jobin M, Burger C, Teneggi V, Buck A. Quantitative cerebral H₂(15)O perfusion PET without arterial blood sampling, a method based on washout rate. *Eur J Nucl Med Mol Imaging*. 2003;30:572–580. doi: [10.1007/s00259-002-1105-x](https://doi.org/10.1007/s00259-002-1105-x)
 10. Ferré JC, Bannier E, Raoult H, Mineur G, Carsin-Nicol B, Gauvrit JY. Arterial spin labeling (ASL) perfusion: techniques and clinical use. *Diagn Interv Imaging*. 2013;94:1211–1223. doi: [10.1016/j.diii.2013.06.010](https://doi.org/10.1016/j.diii.2013.06.010)
 11. Sebök M, van Niftrik CHB, Piccirelli M, Bozinov O, Wegener S, Esposito G, Pangalu A, Valavanis A, Buck A, Luft AR, et al. BOLD cerebrovascular reactivity as a novel marker for crossed cerebellar diaschisis. *Neurology*. 2018;91:e1328–e1337. doi: [10.1212/wnl.00000000000006287](https://doi.org/10.1212/wnl.00000000000006287)
 12. van Niftrik CHB, Sebök M, Wegener S, Esposito G, Halter M, Hiller A, Stippich C, Luft AR, Regli L, Fierstra J. Increased ipsilateral posterior cerebral artery P2-segment flow velocity predicts hemodynamic impairment. *Stroke*. 2021;52:1469–1472. doi: [10.1161/strokeaha.120.032848](https://doi.org/10.1161/strokeaha.120.032848)
 13. Sebök M, van Niftrik CHB, Wegener S, Luft A, Regli L, Fierstra J. Agreement of novel hemodynamic imaging parameters for the acute and chronic stages of ischemic stroke: a matched-pair cohort study. *Neurosurg Focus*. 2021;51:E12. doi: [10.3171/2021.4.Focus21125](https://doi.org/10.3171/2021.4.Focus21125)
 14. Sebök M, van Niftrik CHB, Piccirelli M, Muscas B, Pangalu A, Wegener S, Stippich C, Regli L, Fierstra J. Crossed cerebellar diaschisis in patients with symptomatic unilateral anterior circulation stroke is associated with hemodynamic impairment in the ipsilateral MCA territory. *J Magn Reson Imaging*. 2021;53:1190–1197. doi: [10.1002/jmri.27410](https://doi.org/10.1002/jmri.27410)
 15. Sebök M, van Niftrik CHB, Winkhofer S, Wegener S, Esposito G, Stippich C, Luft A, Regli L, Fierstra J. Mapping cerebrovascular reactivity impairment in patients with symptomatic unilateral carotid artery disease. *J Am Heart Assoc*. 2021;10:e020792. doi: [10.1161/jaha.121.020792](https://doi.org/10.1161/jaha.121.020792)
 16. Nemoto EM, Yonas H, Chang Y. Stages and thresholds of hemodynamic failure. *Stroke*. 2003;34:2–3. doi: [10.1161/01.str.0000041048.33908.18](https://doi.org/10.1161/01.str.0000041048.33908.18)
 17. North American Symptomatic Carotid Endarterectomy Trial. Methods, patient characteristics, and progress. *Stroke*. 1991;22:711–720. doi: [10.1161/01.str.22.6.711](https://doi.org/10.1161/01.str.22.6.711)
 18. Slessarev M, Han J, Mardimae A, Prisman E, Preiss D, Volgyesi G, Ansel C, Duffin J, Fisher JA. Prospective targeting and control of end-tidal CO₂ and O₂ concentrations. *J Physiol*. 2007;581:1207–1219. doi: [10.1113/jphysiol.2007.129395](https://doi.org/10.1113/jphysiol.2007.129395)
 19. van Niftrik CHB, Piccirelli M, Bozinov O, Pangalu A, Fisher JA, Valavanis A, Luft AR, Weller M, Regli L, Fierstra J. Iterative analysis of cerebrovascular reactivity dynamic response by temporal decomposition. *Brain Behav*. 2017;7:e00705. doi: [10.1002/brb3.705](https://doi.org/10.1002/brb3.705)
 20. Sebök M, Niftrik C, Lohaus N, Esposito G, Amki ME, Winkhofer S, Wegener S, Regli L, Fierstra J. Leptomeningeal collateral activation indicates severely impaired cerebrovascular reserve capacity in patients with symptomatic unilateral carotid artery occlusion. *J Cereb Blood Flow Metab*. 2021;41:3039–3051. doi: [10.1177/0271678x211024373](https://doi.org/10.1177/0271678x211024373)
 21. Skaltsa K, Jover L, Fuster D, Carrasco JL. Optimum threshold estimation based on cost function in a multistate diagnostic setting. *Stat Med*. 2012;31:1098–1109. doi: [10.1002/sim.4369](https://doi.org/10.1002/sim.4369)
 22. Ghosh PK. Box-Cox power transformation unconditional quantile regressions with an application on wage inequality. *J Appl Stat*. 2021;48:3086–3101. doi: [10.1080/02664763.2020.1795817](https://doi.org/10.1080/02664763.2020.1795817)
 23. Baron JC, Bousser MG, Rey A, Guillard A, Comar D, Castaigne P. Reversal of focal "misery-perfusion syndrome" by extra-intracranial arterial bypass in hemodynamic cerebral ischemia. A case study with 15O positron emission tomography. *Stroke*. 1981;12:454–459. doi: [10.1161/01.str.12.4.454](https://doi.org/10.1161/01.str.12.4.454)
 24. Derdeyn CP, Videen TO, Yundt KD, Fritsch SM, Carpenter DA, Grubb RL, Powers WJ. Variability of cerebral blood volume and oxygen extraction: stages of cerebral haemodynamic impairment revisited. *Brain*. 2002;125:595–607. doi: [10.1093/brain/awf047](https://doi.org/10.1093/brain/awf047)
 25. Derdeyn CP. Hemodynamics and oxygen extraction in chronic large artery steno-occlusive disease: clinical applications for predicting stroke risk. *J Cereb Blood Flow and Metab*. 2018;38:1584–1597. doi: [10.1177/0271678X17732884](https://doi.org/10.1177/0271678X17732884)
 26. Webster MW, Makaroun MS, Steed DL, Smith HA, Johnson DW, Yonas H. Compromised cerebral blood flow reactivity is a predictor of stroke in patients with symptomatic carotid artery occlusive disease. *J Vasc Surg*. 1995;21:338–344; discussion 344–335. doi: [10.1016/s0741-5214\(95\)70274-1](https://doi.org/10.1016/s0741-5214(95)70274-1)
 27. Vorstrup S, Brun B, Lassen NA. Evaluation of the cerebral vasodilatory capacity by the acetazolamide test before EC-IC bypass surgery in patients with occlusion of the internal carotid artery. *Stroke*. 1986;17:1291–1298. doi: [10.1161/01.str.17.6.1291](https://doi.org/10.1161/01.str.17.6.1291)
 28. Okazawa H, Yamauchi H, Sugimoto K, Toyoda H, Kishibe Y, Takahashi M. Effects of acetazolamide on cerebral blood flow, blood volume, and oxygen metabolism: a positron emission tomography study with healthy volunteers. *J Cereb Blood Flow Metab*. 2001;21:1472–1479. doi: [10.1097/00004647-200112000-00012](https://doi.org/10.1097/00004647-200112000-00012)
 29. Ringelstein EB, Van Eyck S, Mertens I. Evaluation of cerebral vasomotor reactivity by various vasodilating stimuli: comparison of CO₂ to acetazolamide. *J Cereb Blood Flow Metab*. 1992;12:162–168. doi: [10.1038/jcbfm.1992.20](https://doi.org/10.1038/jcbfm.1992.20)
 30. Alpert NM, Eriksson L, Chang JY, Bergstrom M, Litton JE, Correia JA, Bohm C, Ackerman RH, Taveras JM. Strategy for the measurement of regional cerebral blood flow using short-lived tracers and emission tomography. *J Cereb Blood Flow Metab*. 1984;4:28–34. doi: [10.1038/jcbfm.1984.4](https://doi.org/10.1038/jcbfm.1984.4)
 31. Kuhn FP, Warnock G, Schweingruber T, Sommerauer M, Buck A, Khan N. Quantitative H₂(15)O-PET in pediatric Moyamoya disease: evaluating perfusion before and after cerebral revascularization. *J Stroke Cerebrovasc Dis*. 2015;24:965–971. doi: [10.1016/j.jstrokecerebrovasdis.2014.12.017](https://doi.org/10.1016/j.jstrokecerebrovasdis.2014.12.017)
 32. Sobczyk O, Battisti-Charbonney A, Poublanc J, Crawley AP, Sam K, Fierstra J, Mandell DM, Mikulis DJ, Duffin J, Fisher JA. Assessing cerebrovascular reactivity abnormality by comparison to a reference atlas. *J Cereb Blood Flow Metab*. 2015;35:213–220. doi: [10.1038/jcbfm.2014.184](https://doi.org/10.1038/jcbfm.2014.184)
 33. Sobczyk O, Crawley AP, Poublanc J, Sam K, Mandell DM, Mikulis DJ, Duffin J, Fisher JA. Identifying significant changes in cerebrovascular reactivity to carbon dioxide. *AJNR Am J Neuroradiol*. 2016;37:818–824. doi: [10.3174/ajnr.A4679](https://doi.org/10.3174/ajnr.A4679)
 34. Sobczyk O, Sayin ES, Sam K, Poublanc J, Duffin J, Fisher JA, Mikulis DJ. The reproducibility of cerebrovascular reactivity across MRI scanners. *Front Physiol*. 2021;12:668662. doi: [10.3389/fphys.2021.668662](https://doi.org/10.3389/fphys.2021.668662)
 35. Spano VR, Mandell DM, Poublanc J, Sam K, Battisti-Charbonney A, Pucci O, Han JS, Crawley AP, Fisher JA, Mikulis DJ. CO₂ blood oxygen level-dependent MR mapping of cerebrovascular reserve in a clinical population: safety, tolerability, and technical feasibility. *Radiology*. 2013;266:592–598. doi: [10.1148/radiol.12112795](https://doi.org/10.1148/radiol.12112795)
 36. Sayin ES, Schulman J, Poublanc J, Levine HT, Raghavan LV, Uludag K, Duffin J, Fisher JA, Mikulis DJ, Sobczyk O. Investigations of hypoxia-induced deoxyhemoglobin as a contrast agent for cerebral perfusion imaging. *Hum Brain Mapp*. 2022;44:1019–1029. doi: [10.1002/hbm.26131](https://doi.org/10.1002/hbm.26131)
 37. Ogasawara K, Ogawa A. JET study (Japanese EC-IC Bypass Trial). Article in Japanese. *Nihon Rinsho*. 2006;64:524–527.
 38. Kataoka H, Miyamoto S, Ogasawara K, Iihara K, Takahashi JC, Nakagawara J, Inoue T, Mori E, Ogawa A. Results of prospective cohort study on symptomatic cerebrovascular occlusive disease showing mild

- hemodynamic compromise [Japanese Extracranial-intracranial Bypass Trial (JET)-2 study]. *Neurol Med Chir*. 2015;55:460–468. doi: [10.2176/nmc.oa.2014-0424](https://doi.org/10.2176/nmc.oa.2014-0424)
39. Grubb RL Jr, Derdeyn CP, Fritsch SM, Carpenter DA, Yundt KD, Videen TO, Spitznagel EL, Powers WJ. Importance of hemodynamic factors in the prognosis of symptomatic carotid occlusion. *JAMA*. 1998;280:1055–1060. doi: [10.1001/jama.280.12.1055](https://doi.org/10.1001/jama.280.12.1055)
 40. Yamauchi H, Fukuyama H, Nagahama Y, Nabatame H, Ueno M, Nishizawa S, Konishi J, Shio H. Significance of increased oxygen extraction fraction in five-year prognosis of major cerebral arterial occlusive diseases. *J Nucl Med*. 1999;40:1992–1998.
 41. Carlson AP, Yonas H, Chang YF, Nemoto EM. Failure of cerebral hemodynamic selection in general or of specific positron emission tomography methodology?: Carotid Occlusion Surgery Study (COSS). *Stroke*. 2011;42:3637–3639. doi: [10.1161/strokeaha.111.627745](https://doi.org/10.1161/strokeaha.111.627745)
 42. Powers WJ, Clarke WR, Grubb RL Jr, Videen TO, Adams HP Jr, Derdeyn CP. Extracranial-intracranial bypass surgery for stroke prevention in hemodynamic cerebral ischemia: the Carotid Occlusion Surgery Study randomized trial. *JAMA*. 2011;306:1983–1992. doi: [10.1001/jama.2011.1610](https://doi.org/10.1001/jama.2011.1610)
 43. Sebök M, Esposito G, Niftrik C, Fierstra J, Schubert T, Wegener S, Held J, Kulcsár Z, Luft AR, Regli L. Flow augmentation STA-MCA bypass evaluation for patients with acute stroke and unilateral large vessel occlusion: a proposal for an urgent bypass flowchart. *J Neurosurg*. 2022;137:1–9. doi: [10.3171/2021.10.Jns21986](https://doi.org/10.3171/2021.10.Jns21986)
 44. Hall MK, Kea B, Wang R. Recognising bias in studies of diagnostic tests part 1: patient selection. *Emerg Med J*. 2019;36:431–434. doi: [10.1136/emered-2019-208446](https://doi.org/10.1136/emered-2019-208446)
 45. Kea B, Hall MK, Wang R. Recognising bias in studies of diagnostic tests part 2: interpreting and verifying the index test. *Emerg Med J*. 2019;36:501–505. doi: [10.1136/emered-2019-208447](https://doi.org/10.1136/emered-2019-208447)
 46. Goetti R, Warnock G, Kuhn FP, Guggenberger R, O’Gorman R, Buck A, Khan N, Scheer I. Quantitative cerebral perfusion imaging in children and young adults with Moyamoya disease: comparison of arterial spin-labeling-MRI and H(2)[(15)O]-PET. *AJNR Am J Neuroradiol*. 2014;35:1022–1028. doi: [10.3174/ajnr.A3799](https://doi.org/10.3174/ajnr.A3799)
 47. Hammers A, Allom R, Koeppe MJ, Free SL, Myers R, Lemieux L, Mitchell TN, Brooks DJ, Duncan JS. Three-dimensional maximum probability atlas of the human brain, with particular reference to the temporal lobe. *Hum Brain Mapp*. 2003;19:224–247. doi: [10.1002/hbm.10123](https://doi.org/10.1002/hbm.10123)
 48. Li Y, Li M, Zhang X, Yang S, Fan H, Qin W, Yang L, Yuan J, Hu W. Clinical features and the degree of cerebrovascular stenosis in different types and subtypes of cerebral watershed infarction. *BMC Neurol*. 2017;17:166. doi: [10.1186/s12883-017-0947-6](https://doi.org/10.1186/s12883-017-0947-6)